ELSEVIER

Journal of Alloys and Compounds 444–445 (2007) 212–216

Journal of ALLOYS AND COMPOUNDS

www.elsevier.com/locate/jallcom

Evaluation of the nucleation and growth of helium bubbles in aged plutonium

D.W. Wheeler *, P.D. Bayer

AWE, Aldermaston, Reading, Berkshire RG7 4PR, United Kingdom

Received 3 November 2006; received in revised form 9 January 2007; accepted 9 January 2007
Available online 14 January 2007

Abstract

The processes of radioactive decay that take place in plutonium (Pu) can result in the generation of lattice damage and helium (He) bubbles, which can lead to significant changes to its physical, chemical and mechanical properties. As part of efforts to understand the ageing behaviour of Pu, dilatometry has been used to quantify lattice damage and the nucleation and growth of helium bubbles. Pu specimens were subjected to isothermal heat treatments for extended durations followed by metallographic examination in order to study the microstructures. The dilatometry data have enabled lattice damage and He bubble growth to be measured and quantified, as well as the calculation of diffusion coefficient of He in Pu. The values of the diffusion coefficients and activation energies suggest that the diffusion of He in Pu occurs via a vacancy mechanism, while bubble nucleation and growth at elevated temperatures takes place via the process of Ostwald ripening.

Keywords: Actinide alloys and compounds; Diffusion; Metallography; Thermal analysis

1. Introduction

The processes of radioactive decay that take place in plutonium (Pu) can lead to microstructural changes which have the potential to alter its properties with age. These include the evolution of helium (He) and uranium (^{235}U) from the α decay of ^{239}Pu while americium (Am) and neptunium (Np) are generated as a result of the decay of other Pu isotopes [1]. Of these, the most significant products of the decay process are the generation of lattice damage and evolution of He within the material, the magnitudes of which increase with time. The lattice damage is caused by collisions between the α particles and the recoiling U atoms with the Pu lattice, which results in vacancy-interstitial (Frenkel) pairs. Approximately 2500 Frenkel pairs are created by one U atom, although it is thought that up to 70% recombine within 100 ps after the decay of a Pu atom owing to the mobility of the vacancies at room temperature: this process is known as "self-annealing" [2].

In addition to Frenkel pairs, the α particles (He nuclei) also acquire two electrons during their passage through the lattice to form He atoms. Helium has limited solubility in metals but He atoms can readily enter lattice vacancies, which enables them to diffuse through the microstructure. The migration and coalescence of He atoms and vacancies results in the formation of He bubbles, which have been observed using transmission electron microscopy [3].

It has been postulated that, over time, He bubbles, in combination with voids, may cause significant swelling. Wolfer [2] has suggested that such a transition may indeed occur at a future, as yet unknown, juncture; however, he has speculated that it may not occur in Pu that is less than 100 years of age. It is clear that many questions remain to be answered satisfactorily and the present work was undertaken to gain a greater understanding of this phenomenon. As part of efforts to understand the ageing behaviour of Pu, dilatometry has been used to measure He bubble nucleation and growth at elevated temperature and the release of stored energy associated with lattice defect removal.

2. Experimental details

Pu–Ga alloys with Ga contents of between 2.0 and 3.4 at% and between 3 weeks and 31 years of age were subjected to isothermal treatments in a He atmosphere using a Perkin Elmer TMA7 dilatometer. During a test, the specimen is placed inside a fused silica tube, which is mounted vertically within the furnace, and a probe, also made from fused silica, rests on its upper surface. The probe is

* Corresponding author. Tel.: +44 118 982 4891.
E-mail address: David.Wheeler@awe.co.uk (D.W. Wheeler).

0925-8388/$ – see front matter.
doi:10.1016/j.jallcom.2007.01.038

connected to a linear variable displacement transducer (LVDT), which measures any changes to the specimen length during the experiment.

The Pu specimens were between 1.5 and 5.5 mm in length and 1.0 and 3.5 g in weight. The He gas was of commercial purity and was also passed through a titanium (Ti) getter furnace prior to entering the dilatometer as a gas shroud. The He gas flow rate was 30 ml min^{-1}: under these conditions, no weight gain was detected in specimens treated at 300 °C for 100 h (the precision of the balance was ±0.4 mg). At higher temperatures, small weight gains may be observed: as an example, a specimen 1.62 g in weight, which was treated at 500 °C for 72 h, exhibited a weight gain of 1.7 mg. In the present study, in order to minimise the effects of oxidation, the majority of the tests were conducted at temperatures below 300 °C.

In the present tests, the specimens were heated to the treatment temperature at a rate of 10 °C min^{-1} and held there for up to 2 weeks; the treatment temperatures were between 150 and 600 °C. The changes to the specimen dimensions were continuously monitored by the LVDT throughout the tests. In order to validate the accuracy of the equipment, the thermal expansion coefficients of copper (Cu) and tantalum (Ta) specimens were measured, the values of which were consistent with those given in the literature. Following the tests of the Pu specimens, they were mounted in epoxy resin and polished for metallographic examination.

3. Results and discussion

3.1. Evolution and growth of helium bubbles

A typical output from a dilatometry experiment, in which a specimen is subjected to an isothermal hold, is shown in Fig. 1. The graph, which shows the change in probe position with time expressed as normalised length change (d*L*/*L*), contains four distinct stages. The first stage occurs as the specimen heats to temperature and is a function of the thermal expansion coefficient of the material. Once the treatment temperature has been attained, the second stage – contraction of the specimen – may be observed. The length of time over which this contraction occurs is dependent on the test temperature: at 150 °C the contraction was observed to continue for approximately 33 h, while at 400 °C it was only 5 min. As a consequence, these contractions cannot be ascribed to differences in expansion due to temperature gradients within the dilatometer during heating. Instead, it is thought that they have been caused by the annealing-out of the accumulated radiation damage that is present in the lattice (it should be noted that such contractions were not observed in tests of Cu and Ta under the same conditions). Therefore, the magnitude of the radiation damage contraction is a function of the age of the material. This is illustrated in Fig. 2 that shows significantly more contraction of 12-year-old material than new material in the early stages of the treatment. As a result, the extent of this contraction enables the amount of radiation-induced lattice damage to be measured. Dilatometry measurements of Pu specimens from zero to three years of age has indicated that the increase of contraction that can be attributed to lattice damage removal with age reaches a maximum after approximately 2 years with no significant increase observed thereafter: this is thought to be caused by the equalisation of the rates of defect generation and defect removal. At this point, the displaced atoms have been estimated to constitute about 3% of the total number of atoms in the lattice.

The third stage of the graph is the incubation period where no change in volume is observed. During this stage, He bubbles generated by the radioactive decay process and subsequent

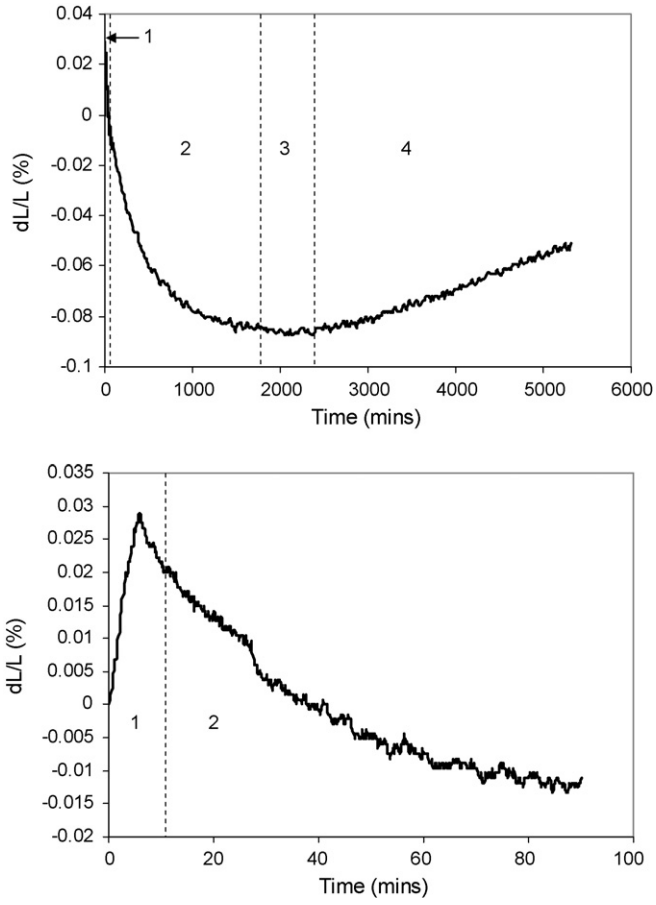

Fig. 1. Dilatometry trace of 3-year-old Pu–2.0 at% Ga heated to 150 °C for 89 h (top) showing the four stages of behaviour: (1) heating; (2) contraction caused by the annealing-out of radiation damage; (3) incubation; and (4) expansion due to He bubble growth. The heating and contraction in the early stages of the test are also shown in greater detail (bottom).

diffusion of He atoms are redistributed from their original network into a new thermodymanically stable embryo network at the test temperature. This process then leads to the fourth stage where subsequent expansion of the material occurs as the embryos grow in size. The rate of He generation is approxi-

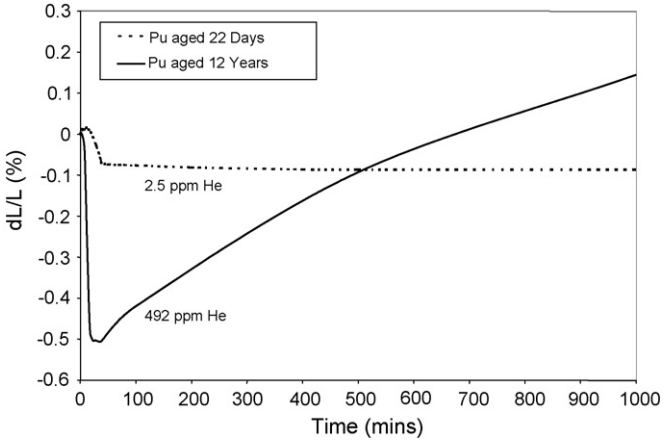

Fig. 2. Dilatometry trace of "new" and 12-year-old Pu–2 at% Ga subjected to an isothermal treatment to 430 °C.

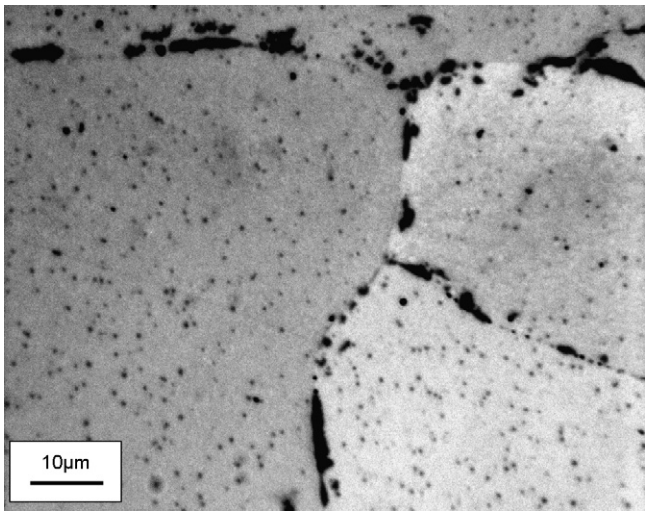

Fig. 3. Optical micrograph of 31-year-old Pu–3.4 at% Ga heated to 300 °C for 306 h. The figure shows a network of micron-sized bubbles distributed throughout the grains.

mately 41 at ppm per year [2]. The amount of expansion during stage four is a function of age: as shown in Fig. 2, the significantly higher levels of He in older material causes it to exhibit expansion once the lattice damage has been annealed out. This is in contrast to the "new" material, where the negligible amount of He is insufficient to cause any detectable expansion.

The bubbles can be seen in optical micrographs of the heat treated material. Fig. 3 shows the presence of a network of submicron sized bubbles, both at the grain boundaries and within the grains themselves. Furthermore, a smaller quantity of much larger sized bubbles can also be observed. They are shown in Fig. 4, which shows micrographs (in both the etched and unetched condition) taken from 31-year-old Pu heated to 300 °C for 306 h. The observation of these features in the unetched condition indicates that their existence cannot be ascribed to the effect of etching the Pu during specimen preparation.

These larger bubbles are similar to "breakaway" bubbles, which have been reported in annealing studies of copper implanted with helium [4,5]. Those findings, derived from both theoretical and empirical studies, indicated that after a swelling threshold is exceeded increased breakaway swelling occurs, leading to the formation of significantly larger bubbles, the sizes

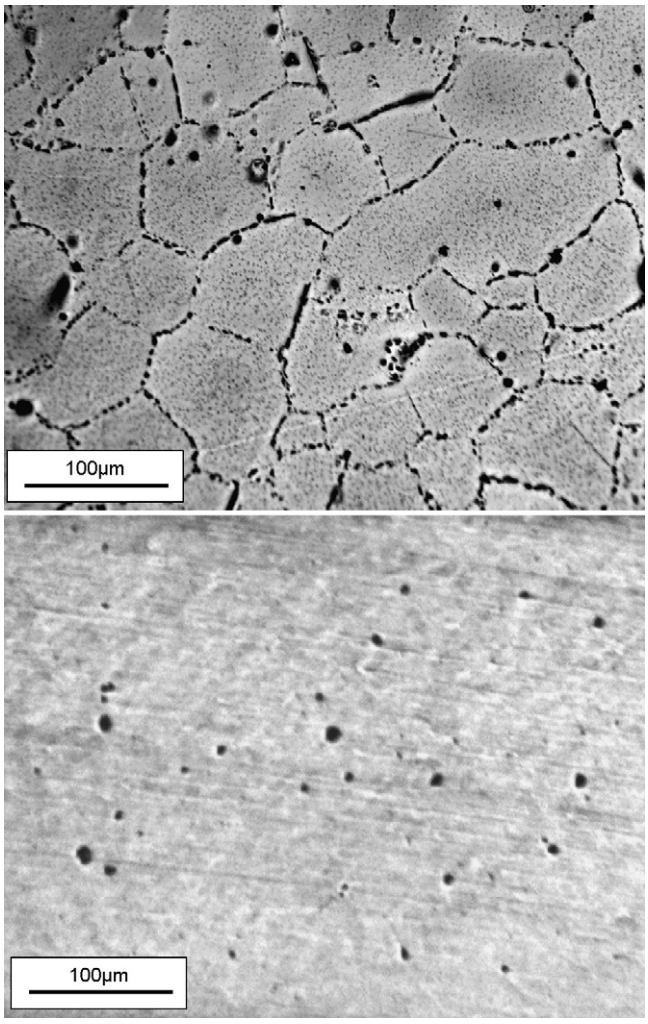

Fig. 4. Optical micrographs of 31-year-old Pu–3.4 at% Ga heated to 300 °C for 306 h in the etched (top) and unetched (bottom) conditions.

of which could not be explained in terms of conventional bubble migration and coalescence theory. Table 1 lists the bubble sizes from each temperature, which were measured from micrographs of metallographic sections taken from the treated specimens. Fig. 5 shows the densities of the two scales of bubbles and their dependence on annealing temperature.

Table 1
Bubble sizes and inter-bubble distances in 31-year aged plutonium

Test conditions	Mean bubble diameter (μm)	Mean bubble separation distance (μm)	Range of breakaway bubble diameters (μm)	Mean breakaway bubble diameter (μm)	Bubble separation distance (μm)
150 °C/167 h	–[a]	–[a]	0.8–10	1	6
200 °C/188 h	–[a]	–[a]	0.9–20	2	10
300 °C/306 h	0.5	3	5–30	10	46
400 °C/16 h	0.7	7	Not seen after 16 h anneal		–
400 °C/363 h	0.8	3.3	7–50	29	80
500 °C/16 h	28	60	Not seen		–
500 °C/336 h	60	60	Bubbles merged to one size		–
600 °C/3 h	30	65	55–80	60	90

From the bubble size and inter-bubble distances the coefficient for helium diffusion can be calculated.
[a] Equilibrium bubbles could not be resolved on these specimens.

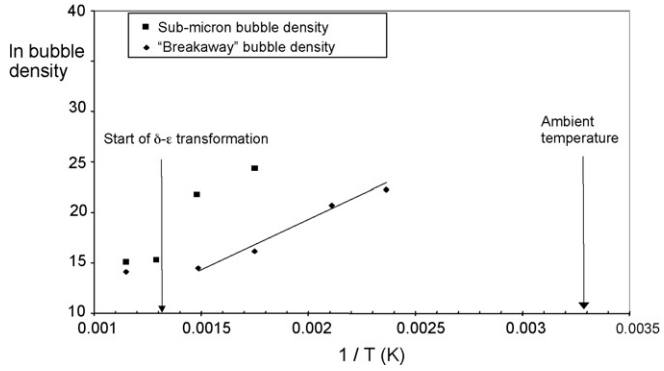

Fig. 5. Graph of bubble density vs. annealing temperature for the equilibrium bubbles and the "breakaway" bubbles in aged Pu heated in the dilatometer.

3.2. Calculation of diffusion coefficients

The data obtained from these experiments (e.g. bubble sizes, bubble densities and interbubble distances) can be used to evaluate the transport of He through the lattice into the new stable equilibrium bubble network from the rate of bubble growth; the diffusion path is half the interbubble distance. By considering the case of diffusion into a hollow sphere from a thick wall, and assuming that the He concentration is uniform throughout the wall, the diffusion coefficient can be calculated using the following equation derived by Barrer [6]:

$$\frac{C}{C_{\mathrm{m}}} = \left[1 - \frac{12}{\pi^2}\sum_{n=1}^{\infty} - \frac{\cos n\pi}{n^2}\exp\left(\frac{-Dn^2\pi^2 t}{(a-b)^2}\right)\right] \quad (1)$$

where a is the sphere radius (in this case half the bubble separation distance), b is the He bubble radius, t is time, D the diffusion coefficient, C is the He concentration in the bubbles and C_{m} the total helium concentration. C can be calculated from bubble sizes and distributions, while C_{m} is known from the age of the material (assuming that the rate of He generation is 41 at ppm per year). Using these parameters, the following series can be expanded:

$$\frac{C}{C_{\mathrm{m}}} = 1 - \frac{12}{\pi^2}(\mathrm{e}^{-z} - \mathrm{e}^{-4z} + \mathrm{e}^{-9z} - \mathrm{e}^{-16z}\cdots) \quad (2)$$

where

$$z = \frac{Dn2\pi^2 t}{(a-b)^2} \quad (3)$$

The values of D, which are obtained by iteration, are plotted in Fig. 6. The activation energies were calculated from the gradients of the two lines. The graph shows that distinctly different diffusivity is observed between normal and breakaway bubbles. The figure also includes a value for D at ambient temperature, derived from analytical data taken from He evolution measurements of a Pu specimen that had been stored at room temperature for 31 years. In those measurements, the He content was below the limit of detection for the equipment; this data point represents a maximum value of diffusion coefficient at this temperature. This indicates that the activation energy (Q) at room temperature is similar to that at elevated temperature: therefore, it can be

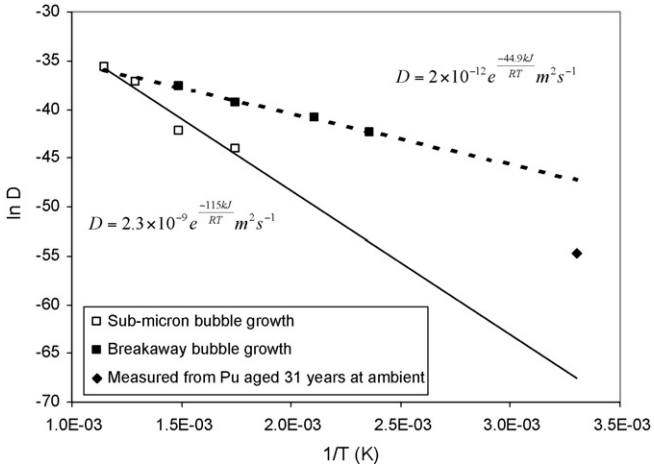

Fig. 6. Graph of diffusion coefficient versus temperature for the diffusion of He in 31-year-old Pu–3.4 at% Ga. The diffusion coefficients were calculated using the Barrer equation. The data point at ambient temperature represents a maximum diffusion coefficient.

inferred that the diffusion mechanism by which the sub-micron bubbles are formed at elevated temperature is also operative at ambient temperature.

By comparison of the apparent activation energy for diffusion as measured in this work with values obtained by measurement and calculation in studies of other face centred cubic (fcc) metals it is possible to infer the likely mechanism by which diffusion of He in Pu takes place. In metals where He diffusion is considered to take place by a vacancy mechanism similar to that in most substitutional sold solutions (e.g. He in Al, Ag or Au) the measured apparent activation energy is close to the self-diffusion energy of the metal [7]. For impeded interstitial migration (i.e. He dissociation from vacancies followed by interstitial diffusion until capture in a larger bubble) the activation energies are low. As an example, an activation energy of 0.81 eV has been measured in Ni, which compares with calculated values for Ni of 0.7 and 2.9 eV for interstitial and vacancy diffusion, respectively [7,8].

In the present study, the apparent activation energy for the formation of the small bubbles has been measured to be 1.24 eV. This is close to the apparent activation energy for Pu self-diffusion of 1.04 eV reported in the literature [9]. This discrepancy can be explained by the presence of more than one atom per vacancy: in the case of Pu, positron annihilation measurements have suggested that there are 2–3 He atoms per vacancy [3]. As a result, the activation energy for diffusion of these vacancies is increased.

It is therefore proposed that the formation and growth of the sub-micron bubbles is by Ostwald ripening in which the network of bubbles formed at ambient temperature dissociates and the He atoms contained therein diffuse by vacancy migration into a network that is thermodynamically stable at higher temperature. Such a mechanism is expected to be dominant at elevated temperature and/or at low He concentration [10].

For the breakaway bubbles the apparent activation energy is 0.48 eV, which suggests that they are formed by a different mechanism, for example an impeded interstitial mechanism for He diffusion. It is clear that vacancy and interstitial mechanisms

cannot both operate independently at the same time. However, Escobar Galindo et al. [5] noted that breakaway bubble growth was only observed once a swelling threshold had been exceeded. Therefore, breakaway bubbles form at a later stage in the process at the expense of vacancy diffusion. It is possible for agglomeration of bubbles to occur by surface diffusion of Pu, thereby conferring mobility to the bubbles. However, this is only thought to be possible with very small bubbles having diameters on the nanometre scale, not that of the micron scale as measured in this study. As the bubbles agglomerate to larger sizes, and the new bubble density is established at temperature, more atoms are required to be transported to allow the bubble to move. Eventually random diffusion will render the bubble immobile.

4. Conclusions

Extended isothermal heat treatments of aged Pu at elevated temperatures have shown that two ageing processes in Pu – the generation of lattice damage and the evolution of He – can be measured and quantified using dilatometry. Initially, annealing of the lattice damage occurs, which causes contraction of the material. This is followed by He agglomeration, which leads to expansion of the material caused by bubble growth.

Examination of heat-treated Pu specimens has revealed the presence of two scales of He bubbles: sub-micron-sized bubbles and "breakaway" bubbles. The latter have also been seen in He-implanted Cu, most commonly near interfaces and at sites where diffusion is enhanced, for example grain boundaries. Diffusion measurements and calculations suggest that He migration primarily occurs by a vacancy mechanism. This continues until a subsequent, as yet unknown, threshold is exceeded, which leads to this mechanism being augmented by an impeded interstitial mechanism causing breakaway bubble growth. It may be possible that bubble migration and agglomeration by surface diffusion may occur with nanometre-sized bubbles; however, such a mechanism is not thought to explain the formation of the micron-sized bubbles observed.

References

[1] S.S. Hecker, J.C. Martz, in: L.G. Mallinson (Ed.), Proceedings of the International Conference on Ageing Studies and Lifetime Extension of Materials, Kluwer Academic Publishers, 1999, pp. 23–52.
[2] W.G. Wolfer, Los Alamos Sci. 26 (2000) 274–285.
[3] A.J. Schwartz, M.A. Wall, T.G. Zocco, W.G. Wolfer, Philos. Mag. 85 (2005) 479–488.
[4] J.H. Evans, J. Nucl. Mater. 334 (2004) 40–46.
[5] R. Escobar Galindo, A. van Veen, J.H. Evans, H. Schut, J.T.M. de Hosson, Nucl. Instrum. Methods Phys. Res., Sect. B 217 (2004) 262–275.
[6] R.M. Barrer, Diffusion in and through Solids, Cambridge University Press, 1951.
[7] H. Ullmaier, Nucl. Fusion 24 (1984) 1039–1083.
[8] P. Jung, K. Schroeder, J. Nucl. Mater. 155–157 (1988) 1137–1141.
[9] R.D. Nelson, in: O.J. Wick (Ed.), Plutonium Handbook, American Nuclear Society, 1980, pp. 125–126.
[10] H. Trinkaus, B.N. Singh, J. Nucl. Mater. 323 (2003) 229–242.